

Acid is Key to the Radical-Trapping Antioxidant Activity of Nitroxides

Supporting Information

Evan A. Haidasz,[‡] Derek Meng,[‡] Riccardo Amorati,[¶] Andrea Baschieri,[¶] Keith U. Ingold,[§]

Luca Valgimigli^{¶*} and Derek A. Pratt^{‡*}

[‡]*Department of Chemistry, University of Ottawa, Ottawa, Ontario K1N 6N5, Canada,*

[¶]*Department of Chemistry “G. Ciamician”, University of Bologna, Bologna, I-40126, Italy, and*

[§]*National Research Council of Canada, Ottawa, Ontario K1A 0R6, Canada.*

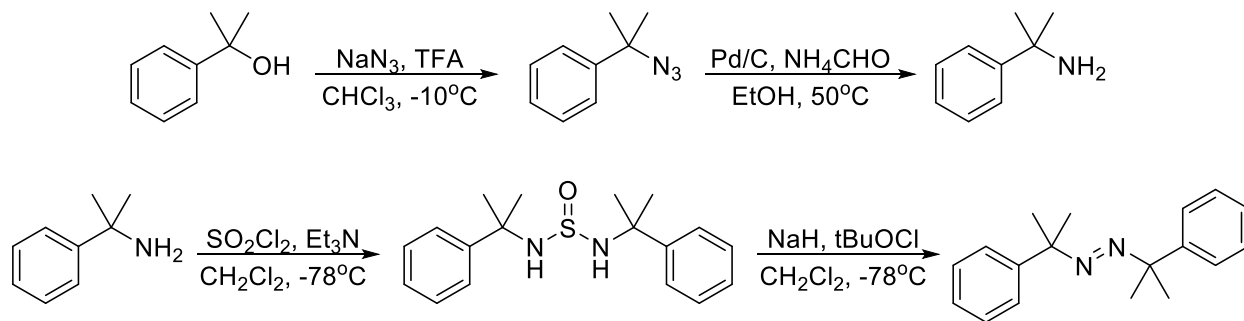
dpratt@uottawa.ca, luca.valgimigli@unibo.it

Table of Contents

Synthetic Procedures	S2
Model Reaction Data	S4
TEMPO ⁺ BF ₄ ⁻ Reactions Monitored by UV-Vis Spectroscopy	S6
Inhibited Autoxidations	S8
EPR Experiments	S13
High Temperature Autoxidation Data	S16
CBS-QB3 Computational Results and Structures	S18
References	S22

Synthetic Procedures

Azocumene. Azocumene was synthesized via the procedure reported by Ikeda,¹ and as had been previously synthesized by our lab.²



To a solution of cumyl alcohol (10 mmol) and sodium azide (22 mmol) in 10 mL CHCl_3 cooled to -10°C was added TFA (55 mmol) dropwise as a solution in 10 mL CHCl_3 . The solution was stirred overnight and upon reaction completion (by TLC) was quenched with water. Following extraction with CH_2Cl_2 , the organics were washed with brine, dried over MgSO_4 , and concentrated. The crude cumylazide was then dissolved in 50 mL EtOH and ammonium formate (50 mmol) and 10% Pd/C (100 mg) were added. The reaction was stirred at 50°C overnight. Upon completion, the solution was diluted with ether and filtered through a pad of silica to afford cumylamine as a pale yellow oil. Yield: 72%. Spectral data were consistent with those in the literature.¹

To a solution of cumylamine (10 mmol) and dry Et_3N (11 mmol) in dry CH_2Cl_2 (10 mL) cooled to -78°C was added sulfuryl chloride (5.1 mmol) dropwise. The reaction was maintained at -78°C until completion, as determined by TLC. The reaction was quenched by addition of water, extracted with CH_2Cl_2 and the organics were washed with brine, dried over MgSO_4 , and concentrated. Recrystallization from EtOH afforded white needles. Yield: 71%. Spectral data were consistent with those in the literature.¹

To a suspension of NaH (2.1 mmol) in dry THF cooled to 0°C was added N,N-bis(1-methyl-1-phenethyl)-sulfamide (3, 1.0 mmol) as a solution in THF dropwise. After 2 hours, the solution was cooled to -78°C and tert-butylhypochlorite (1.1 mmol) was added dropwise. The solution was allowed to warm to room temperature and then quenched with water and extracted with Et_2O . Organics were washed with brine, dried over MgSO_4 , and concentrated. Purification by column chromatography (Pet Ether/ Et_2O) afforded azocumene which was then further purified by recrystallization from Hexanes/ CH_2Cl_2 at -20°C . Yield 11%. Spectral data were consistent with those in the literature.¹

Azobis(1-phenylethane). The title compounds was synthesized by a modified version of a literature procedure.^{14,15} Briefly, acetophenone (12 mL, 100 mmol) and hydrazine hydrate (2.5 mL, 50 mmol) were dissolved in 50 mL of EtOH , *p*-toluenesulfonic acid (190 mg, 1.0 mmol) was added and the mixture was refluxed for 3 hours. Upon cooling to room temperature, a light yellow precipitate had formed. The precipitate was filtered and dried under vacuum, giving 10.2 g of pure acetophenone azine. Yield 86%.

Acetophenone azine (7.0 g, 4.2 mmol), Pd/C (350 mg) and EtOH (45 mL) were combined in a high pressure hydrogenation apparatus, which was then purged with nitrogen, and pressurized to 1500 psi with hydrogen. The reaction was stirred and heated to 50°C for 2 hours, filtered through Celite and concentrated to give 6.2 g of crude bis(1-phenethyl)hydrazine. Yield 89%.

The crude bis(1-phenethyl)hydrazine (6.2 g, 26 mmol) was dissolved in *n*-heptane (100 mL) and oxygen gas was bubbled through the solution until the reaction was complete by TLC. The solvent was removed (not heating past 30°C) and the crude product was purified by column chromatography (eluting with 5% EtOAc/Hexanes) and then recrystallized from MeOH to give 3.0 g of azobis(1-phenylethane). Yield 48%. Spectral data were consistent with those in the literature.¹⁵

TEMPO⁺BF₄⁻. TEMPO⁺BF₄⁻ was synthesized through the procedure of Holan and Jahn.³ Isoamyl nitrite (1.0 mmol) was added slowly to a solution of BF₃-OEt₂ (1.3 mmol) in dry Et₂O (4.5 mL) under argon. The solution was stirred 5 minutes before a solution of TEMPO (156 mg) in 0.5 mL Et₂O was added dropwise over 20 minutes. The solution was stirred an additional 10 minutes. The precipitate was filtered, washed thoroughly with Et₂O, and dried under vacuum. Yield 42%.

4,4'-[(1,10-dioxo-1,10-decanediyl)bis(oxy)]bis[2,2,6,6-tetramethyl-1-oxo-piperidinium] tetrafluoroborate. The oxidation of nitroxide **2** to its corresponding oxoammonium salt was accomplished by an identical procedure to that shown above for the preparation of TEMPO⁺BF₄⁻. The yellow oily solid thus obtained was rinsed thoroughly with diethyl ether, and solidified completely under vacuum overnight. It was stored under vacuum until immediately before use. Spectral data are consistent with reported data for the nitrate salt.¹² FT-IR (ATR): 2931, 1463, 1387, 1235, 1167, 1060 (oxoammonium salt); 1729 (ester), 984 (nitroxide).

Cumyl-TEMPO. Azocumene (1.5 mmol) and TEMPO (3.0 mmol) were dissolved in thoroughly degassed MeCN (15 mL). The solution was stirred at 50°C, under argon, for 24h. The solvent was removed under vacuum, and the residue purified by column chromatography with Et₂O/hexanes to yield a white solid. Yield: 69%. Spectral data are consistent with those in the literature.⁴

1-Phenethyl-TEMPO. The compound was synthesized through the literature procedure. Spectral data are consistent with those in the literature.¹³

Model Reaction Data

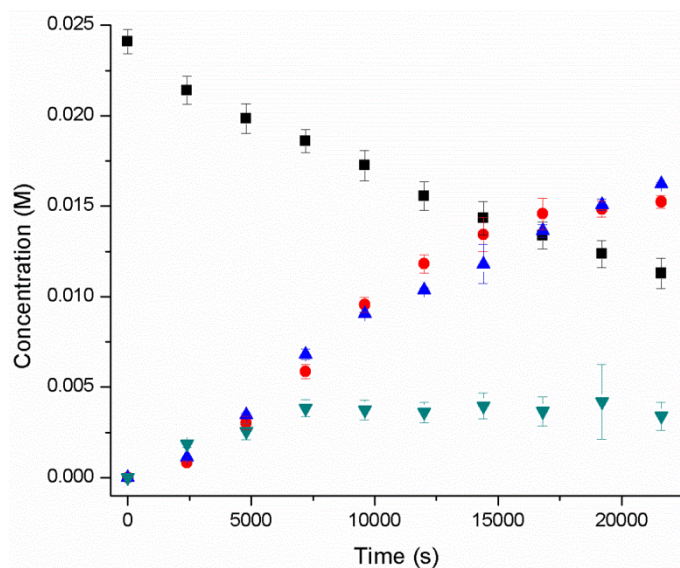


Figure S1. Decomposition of azocumene (■) and formation of the TEMPO-cumyl adduct in the reaction of azocumene (25 mM) and $\text{TEMPO}^+\text{BF}_4^-$ (25 mM) in the presence of $\text{Me}_4\text{N}^+\text{AcO}^-$ (25 mM) in acetonitrile at 50°C under argon with no additive (●), 25 mM AcOH (▲) or 25 mM TFA (▼). Concentrations were determined by HPLC as described in the Experimental Section.

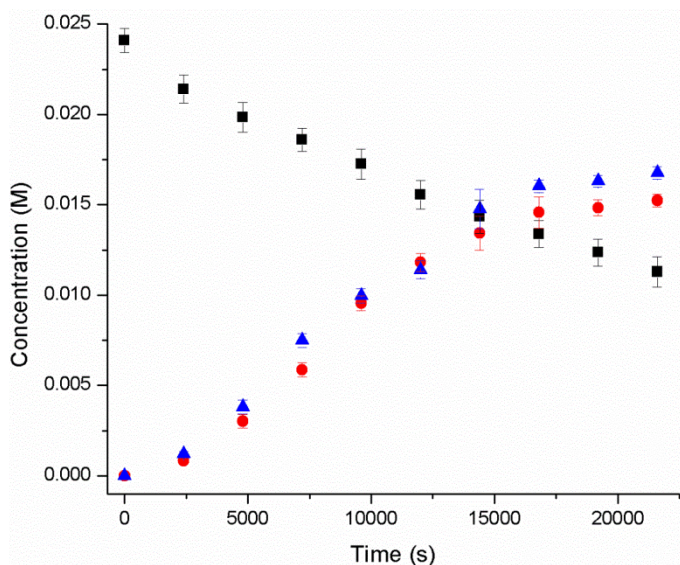


Figure S2. Decomposition of azocumene (■) and formation of the TEMPO-cumyl adduct in the reaction of azocumene (25 mM) and $\text{TEMPO}^+\text{BF}_4^-$ (25 mM) in the presence of $\text{Me}_4\text{N}^+\text{AcO}^-$ (25 mM) at 50°C under argon in acetonitrile (●) or chlorobenzene (▲). Concentrations were determined by HPLC as described in the Experimental Section.

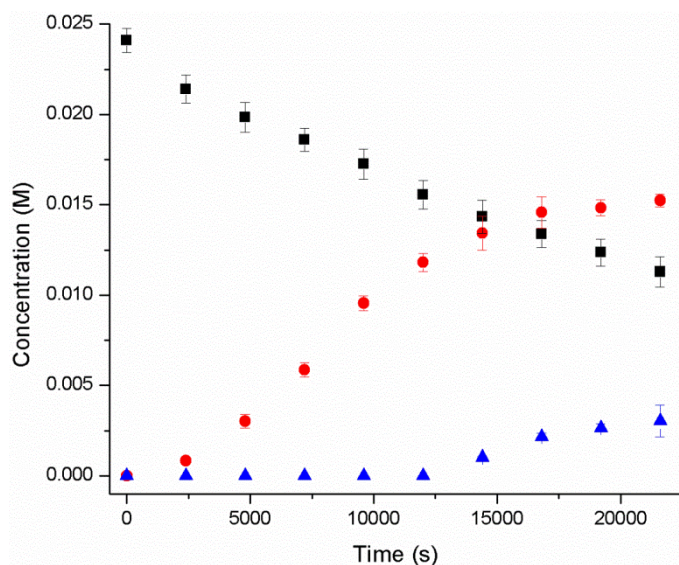


Figure S3. Decomposition of azocumene (■) and formation of the TEMPO-cumyl adduct in the reaction of azocumene (25 mM) and TEMPO⁺BF₄⁻ (25 mM) at 50°C under argon in acetonitrile in the presence (●) or absence (▲) of 25 mM Me₄N⁺AcO⁻. Concentrations were determined by HPLC as described in the Experimental Section.

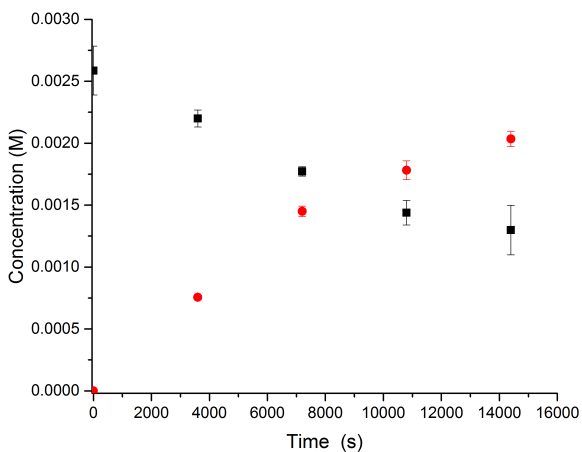


Figure S4. Decomposition of azobis(1-phenylethane) (■) and formation of the TEMPO-phenethyl adduct (●) in the reaction of azobis(1-phenylethane) (25 mM) and TEMPO⁺BF₄⁻ (25 mM) at 100°C under nitrogen in chlorobenzene in the presence of 25 mM Me₄N⁺AcO⁻. Concentrations were determined by HPLC as described in the Experimental Section.

TEMPO⁺BF₄⁻ Reactions Monitored by UV-Vis Spectroscopy

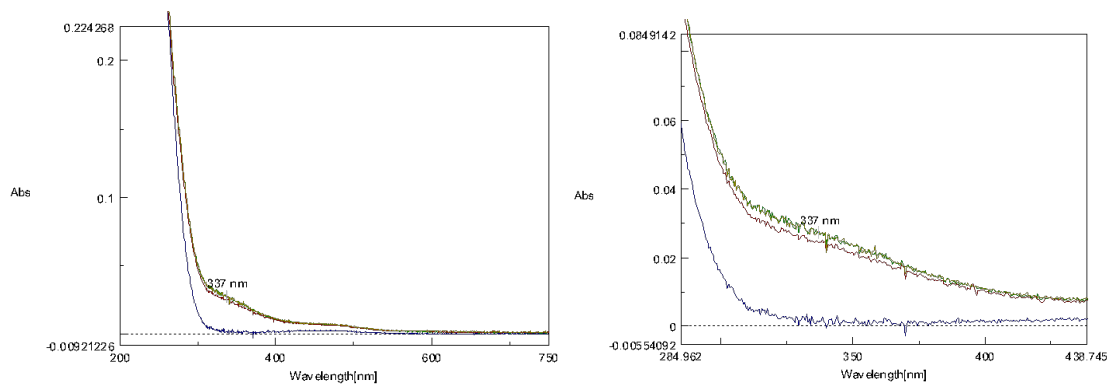


Figure S5. UV-Vis spectra in acetonitrile at 20°C of the mixture of TEMPO⁺BF₄⁻ (0.2 mM) and *tert*-butyl hydroperoxide (3.3 mM) immediately after mixing (green) and after 137 minutes (red). The blue line shows the spectra of a reference solution of TEMPO (0.2 mM) in acetonitrile.

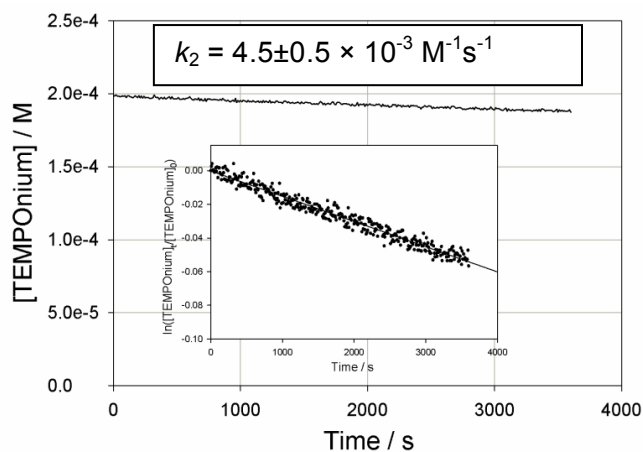


Figure S6. Reaction of TEMPO⁺BF₄⁻ (0.2 mM) with *tert*-butyl hydroperoxide (3.3 mM) in acetonitrile at 20°C monitored at 337 nm. The first-order signal decay is shown in the insert.

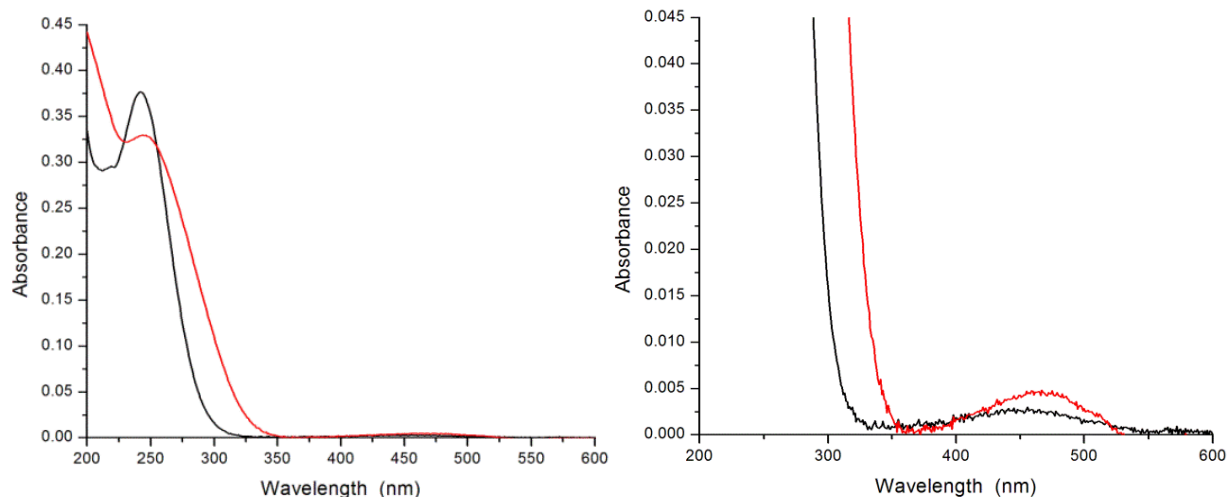


Figure S7. UV-Vis spectra of 0.4 mM TEMPO (black) and TEMPO⁺BF₄⁻ (red) in acetonitrile at 50°C.

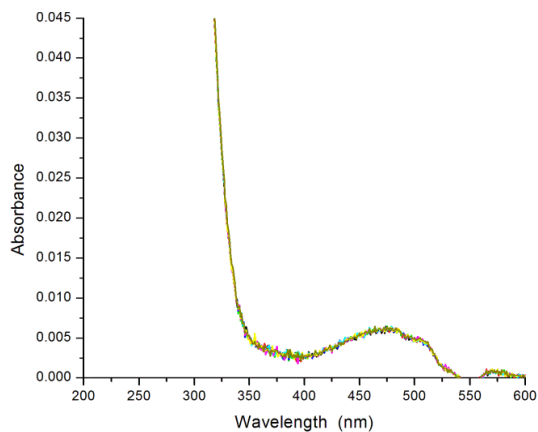


Figure S8. Incubation of TEMPO⁺BF₄⁻ (0.4 mM) in 1% H₂O/MeCN with TFA (10 mM) for 200 minutes (green through pink, indistinguishable).

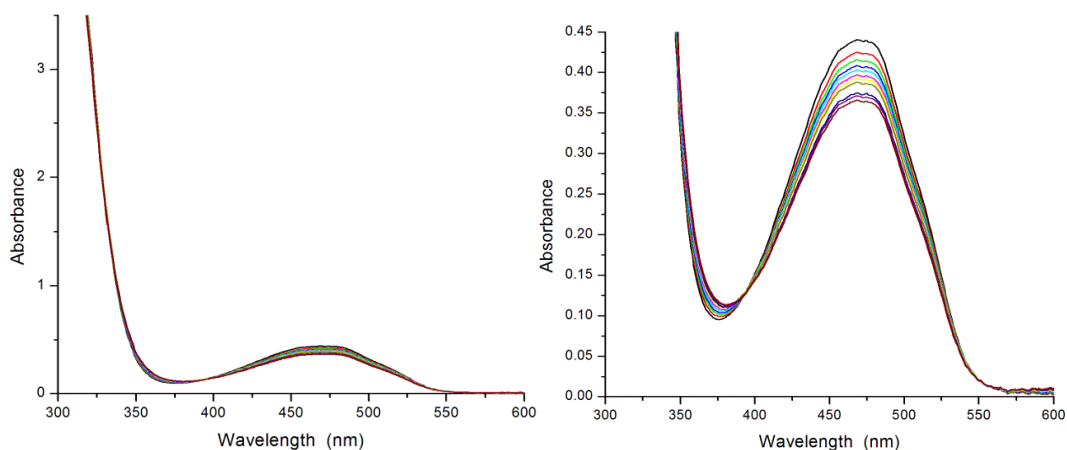


Figure S9. UV-Vis spectra of the decomposition of $\text{TEMPO}^+\text{BF}_4^-$ (20 mM) in 1% $\text{H}_2\text{O}/\text{MeCN}$ containing 0.1 M TFA, at 70°C . Spectra were taken every 4 minutes over the course of 40 minutes and yielded a decomposition rate of $R = 1.3 \times 10^{-6} \text{ Ms}^{-1}$.

Inhibited Autoxidations

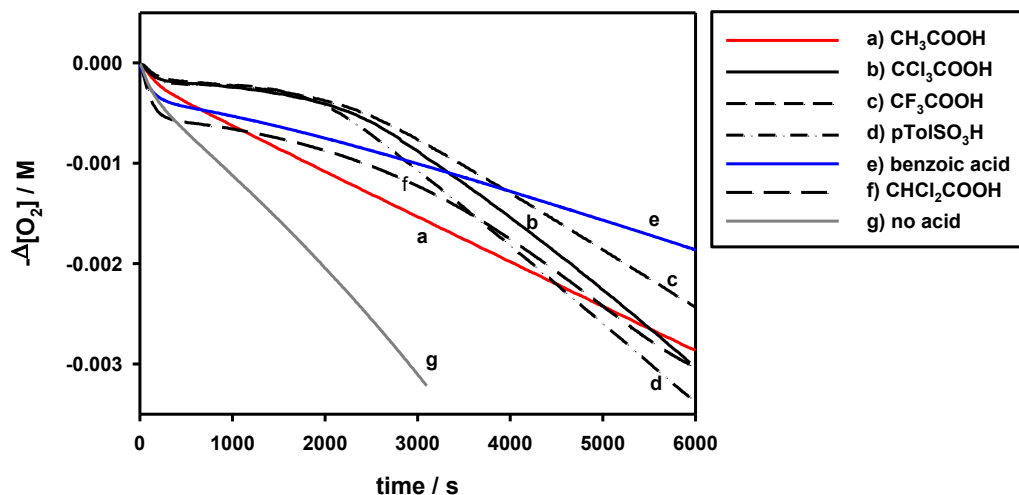


Figure S10. Oxygen consumption plots measured during the autoxidation of styrene (4.3 M) in MeCN (+1% H_2O) initiated by AIBN (0.05 M) at 30°C in the presence of TEMPO ($13 \mu\text{M}$) and 4.3 mM of various acids.

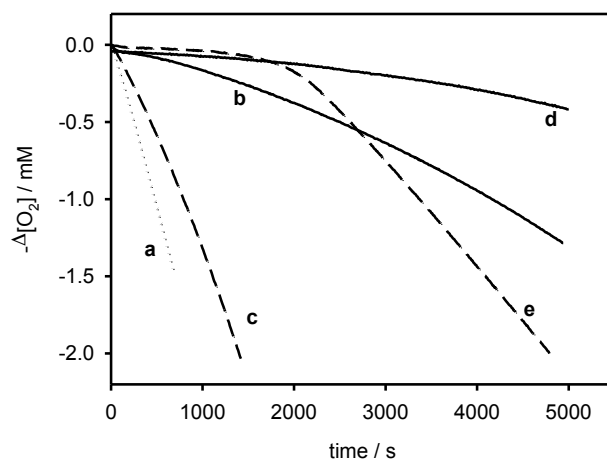


Figure S11. Inhibited autoxidation of styrene (4.3 M) initiated by AIBN (0.05 M) in MeCN with 1% H₂O in (a) the absence of inhibitors, and in the presence of 13 μM of either TEMPO⁺BF₄⁻ (b and c) or TEMPO (d and e) with added acetic acid (43 mM, solid lines) or trifluoroacetic acid (32 mM, dashed lines).

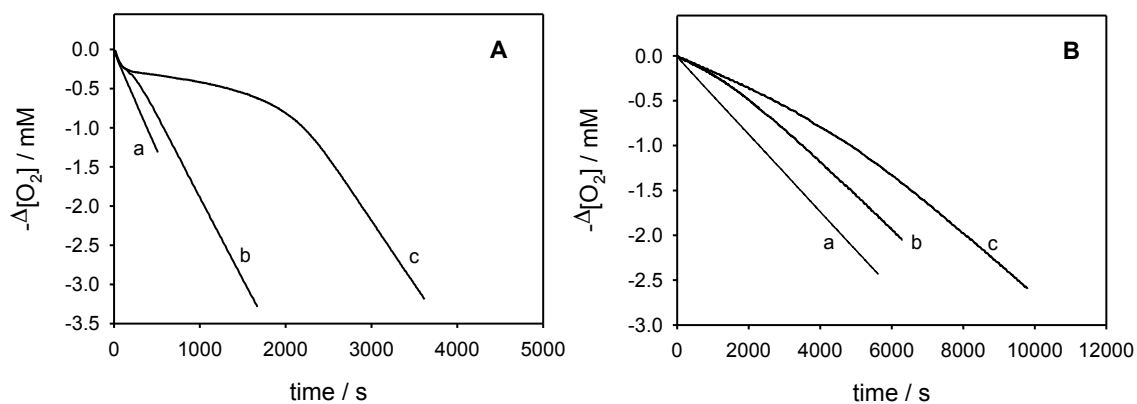
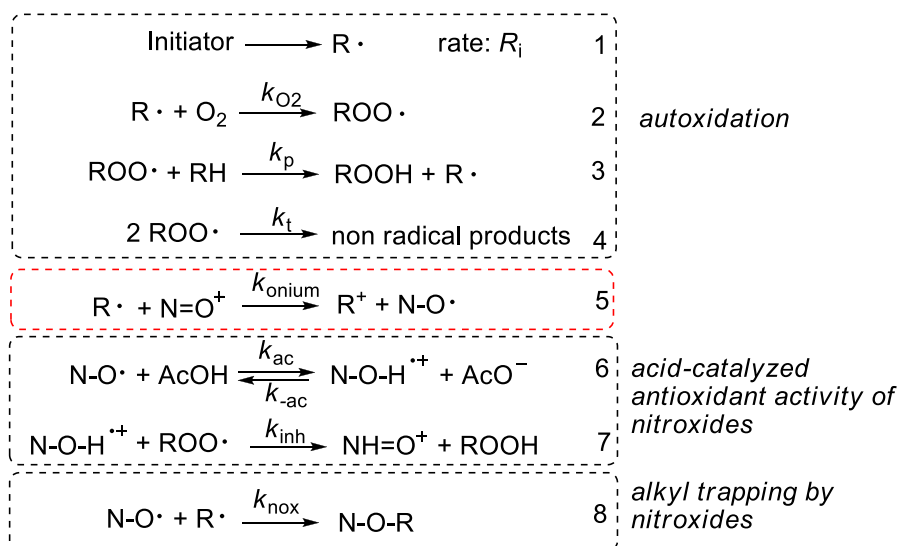


Figure S12. Oxygen consumption observed during the autoxidation of styrene (panel A) or of cumene (panel B) initiated by AIBN (0.05 M) at 30°C using in chlorobenzene. a) without inhibitors; b) TEMPO⁺BF₄⁻ (13 μM) and AcOH (44 mM); c) TEMPO (13 μM) and AcOH (44 mM).

The O₂ consumption plots were analyzed on the basis of the mechanism reactions 1-8 by using Gepasi software⁵ (see Figure S13).



This procedure afforded the value of k_{onio} (reaction 5) and the equilibrium constant k_{ac}/k_{-ac} (reaction 6).

The rate constants for reactions 3 and 4 were from the literature ($k_p = 41 \text{ M}^{-1}\text{s}^{-1}$, $2k_t = 4.2 \times 10^7 \text{ M}^{-1}\text{s}^{-1}$)⁶, while the rate of initiation R_i was experimentally determined as $6.1 \times 10^{-9} \text{ Ms}^{-1}$ by using PMC as reference antioxidant. The reaction of styryl radicals with O₂ in MeCN was set equal to that of benzyl radicals with O₂ ($3.42 \times 10^9 \text{ M}^{-1}\text{s}^{-1}$)⁷, the backward reaction 6 was fixed at the diffusion controlled limit ($k_{-ac} = 5 \times 10^9 \text{ M}^{-1}\text{s}^{-1}$)⁸, while reaction 8 was fixed to $4.9 \times 10^8 \text{ M}^{-1}\text{s}^{-1}$, as reported for benzyl radicals and TEMPO⁹. The reaction between protonated nitroxide and peroxy radicals k_{inh} (reaction 7) was set equal to $2 \times 10^8 \text{ M}^{-1}\text{s}^{-1}$ on the basis of our previous results (the highest measured rate constant was $1.8 \times 10^8 \text{ M}^{-1}\text{s}^{-1}$ with 10 mM TSA).¹⁰ The concentration of oxygen was calculated from the known solubility at 30 °C as $[O_2] = 1.8 \text{ mM}$.

The results of the fittings of the autoxidations of styrene inhibited by TEMPO and TEMPOonium in the presence of different concentrations of acetic acid afforded $k_{onium} = (2.4 \pm 0.4) \times 10^{10} \text{ M}^{-1}\text{s}^{-1}$ and $k_{ac}/k_{-ac} = (1.3 \pm 0.6) \times 10^{-6}$. The rate constants k_{onium} are similar to those reported for the reaction of Ar₂CH⁺ and bromide in MeCN ($2 \times 10^{10} \text{ M}^{-1}\text{s}^{-1}$).¹¹

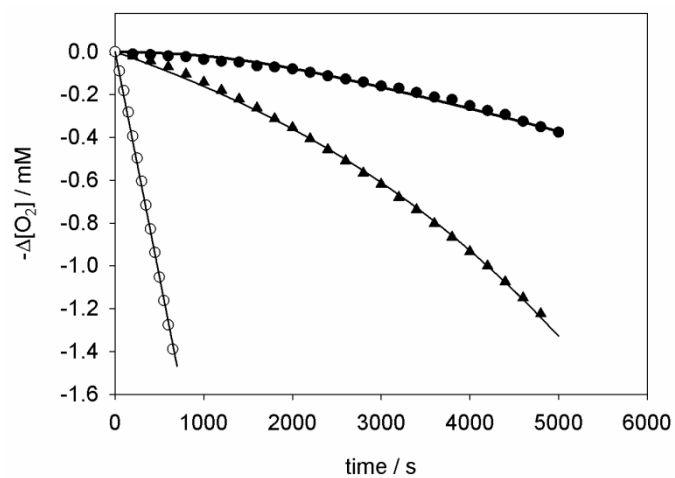


Figure S13. Inhibited autoxidation of styrene (4.3 M) initiated by AIBN (0.05 M) in MeCN with 1% of water and acetic acid (0.043 M), in the absence of inhibitors (○) or in the presence of TEMPO (13 μ M, ●) or TEMPO⁺ (13 μ M, ▲). Lines represent the results from numerical fittings, see text.

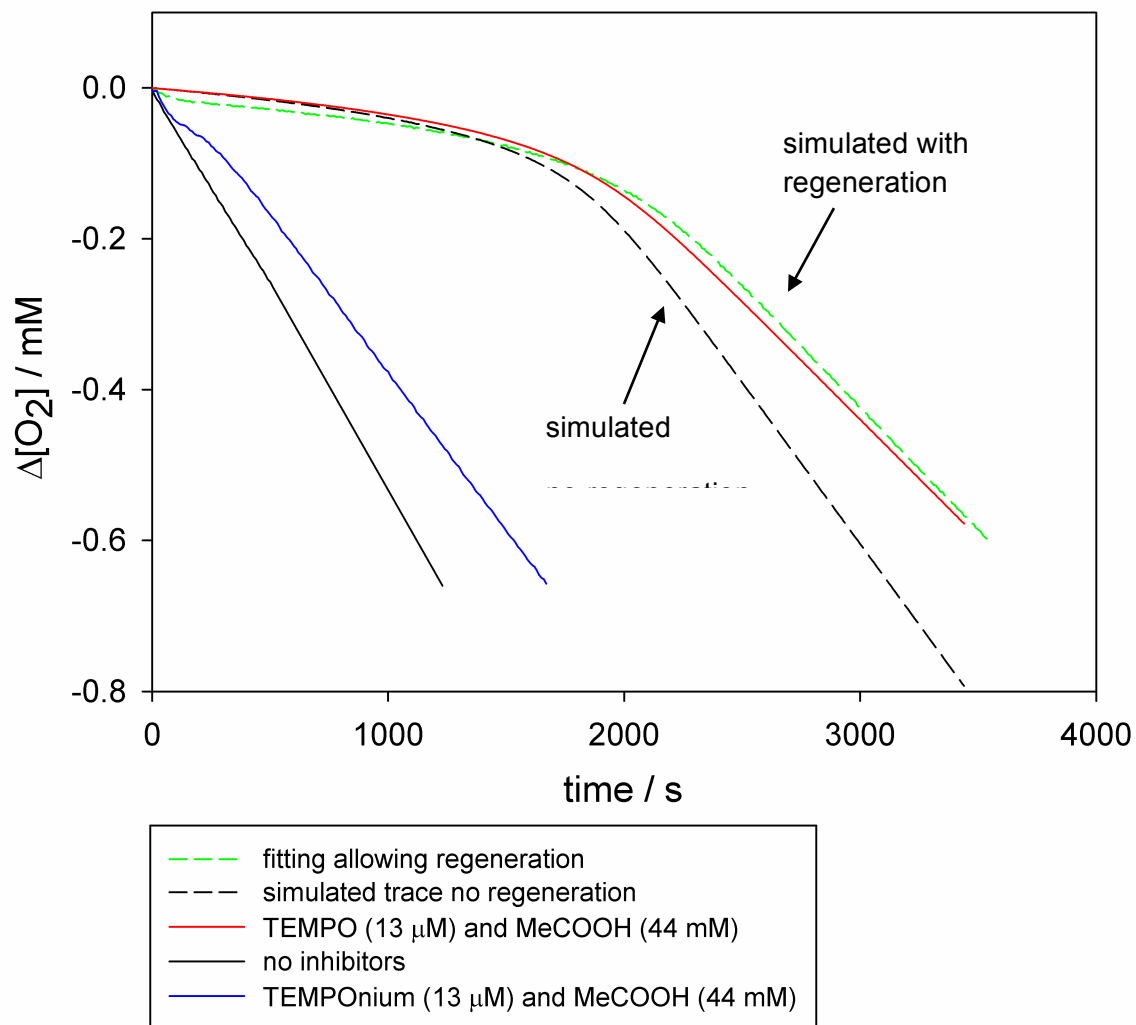


Figure S14. Oxygen uptake plots recorded during the autoxidation of styrene (50% v/v) in chlorobenzene, initiated by AIBN 0.05M at 303K, in the absence of inhibitors or in the presence of 13 μM TEMPO + 44 mM acetic acid or 13 μM TEMPO⁺BF₄⁻ + 44 mM acetic acid as indicated in the legend. Simulated traces impose no regeneration of TEMPO from TEMPO⁺ (black) or allow for regeneration (green). Best fittings afforded k_{reg} ($= k_{\text{onium}}$) = $1\text{-}2 \times 10^9 \text{ M}^{-1}\text{s}^{-1}$.

EPR Experiments

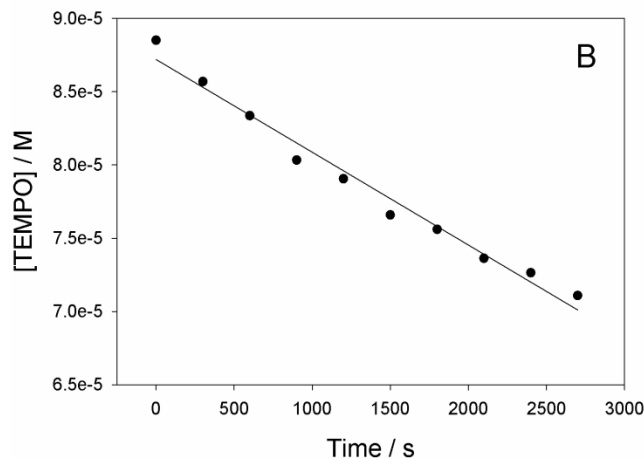


Figure S15. TEMPO concentration determined by EPR during the autoxidation (at 303 K initiated by AIBN 0.05 M) of 40% (v/v) cumene in acetonitrile in the presence of $\text{TEMPO}^+\text{BF}_4^-$ (0.66 mM) upon addition of 26 mM trifluoroacetic acid after ~ 0.1 mM TEMPO had already been formed.

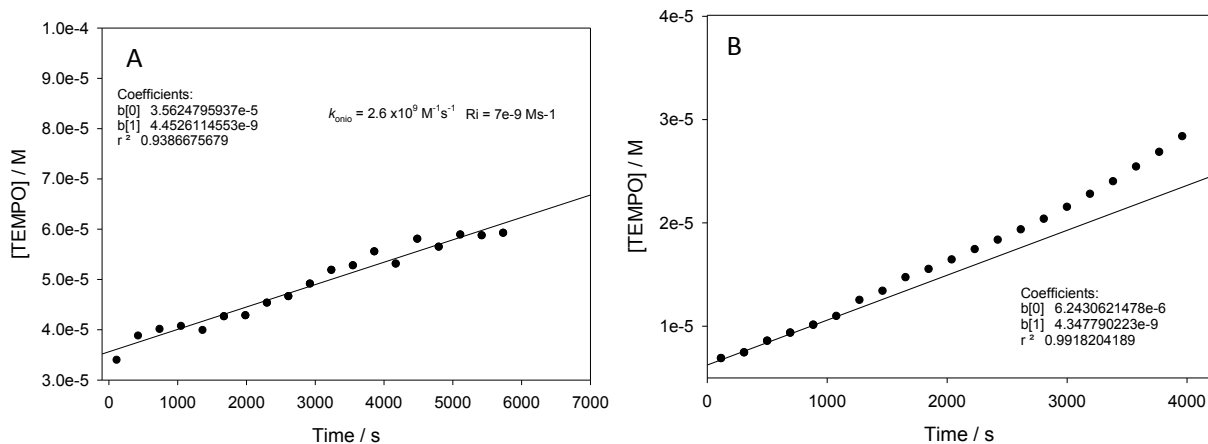


Figure S16. TEMPO concentration determined by EPR during the autoxidation of 40% (v/v) cumene in chlorobenzene at 303 K initiated by AIBN 0.055M in the presence of $\text{TEMPO}^+\text{BF}_4^-$ (1.1 mM) in the presence of 35 mM acetic acid (A) or without acid (B). In the absence of acid, the initial rate is noticeably slower and nonlinear – increasing with time, perhaps due to depletion of O_2 over the longer period of time, improving the competition with alkyl radicals.

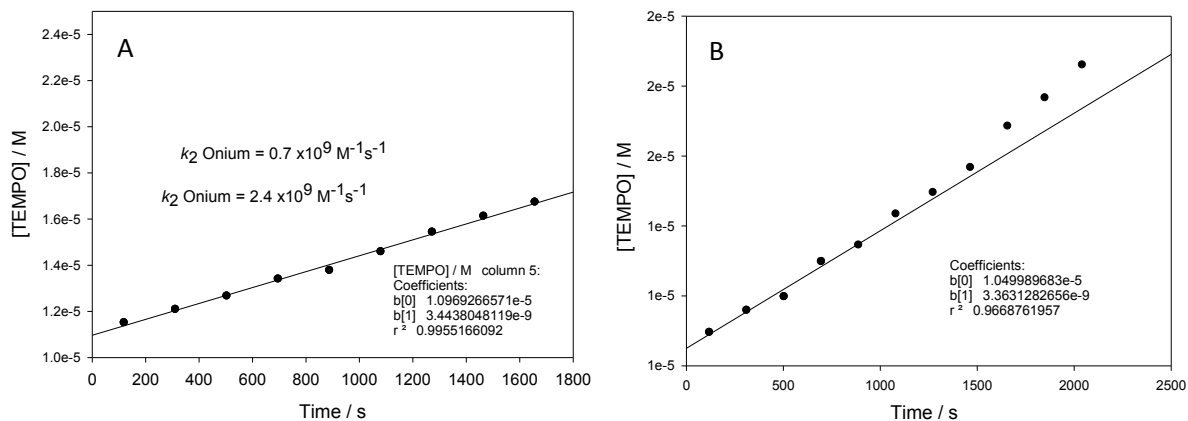


Figure S17. TEMPO concentration determined by EPR during the autoxidation (at 303 K initiated by AIBN 0.055 M) of 45% (v/v) cumene in chlorobenzene in the presence of $\text{TEMPO}^+\text{BF}_4^-$ (0.67 mM) in the presence of 35 mM acetic acid (A) or without acid (B).

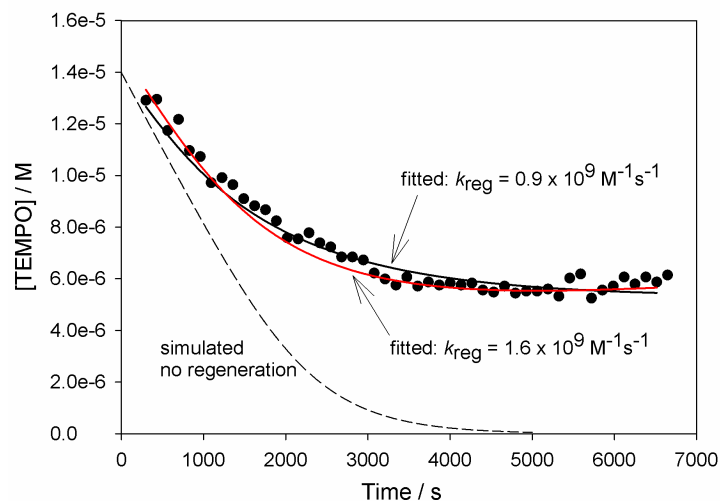


Figure S18. TEMPO concentration determined by EPR during the autoxidation of cumene (45 % v/v) in chlorobenzene initiated by AIBN 0.05M at 303K, in the presence of TEMPO $1.4 \times 10^{-5} \text{ M}$ and acetic acid 52 mM. Simulations show the expected decay in the absence of TEMPO regeneration from TEMPO^+ , and the fitted traces allowing regeneration with the indicated k_{reg} ($= k_{\text{onium}}$).

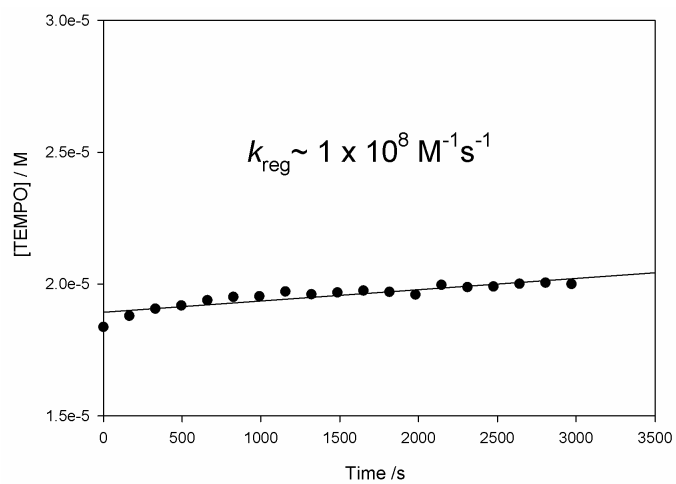


Figure S19. TEMPO concentration determined by EPR during the decomposition of AIBN (0.05 M, $R_i = 6.3 \times 10^{-9} \text{ Ms}^{-1}$) in the presence of $\text{TEMPO}^+\text{BF}_4^-$ (3.5 mM) at 303 K in MeCN.

High Temperature Autoxidations

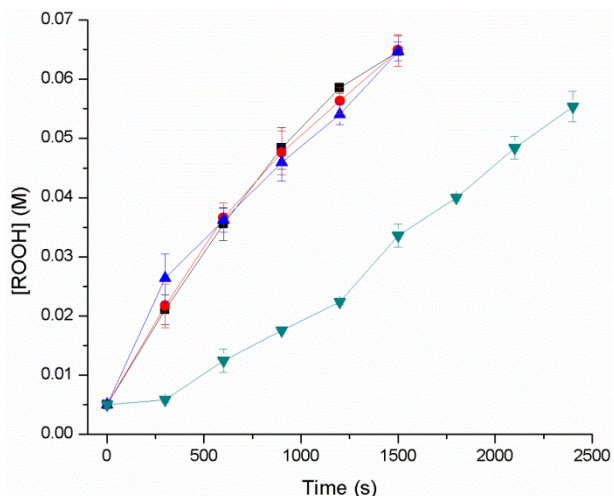


Figure S20. Hydroperoxide formation during the inhibited autoxidation of light paraffin oil at 160°C, initiated by 5.0 mM tetralin hydroperoxide, uninhibited without additives (■), or with 40 mM 2,4,6-tri-*tert*-butylpyridine (●), 40 mM palmitic acid (▲) or inhibited with 40 μM bis(nitroxide) 2 (▼).

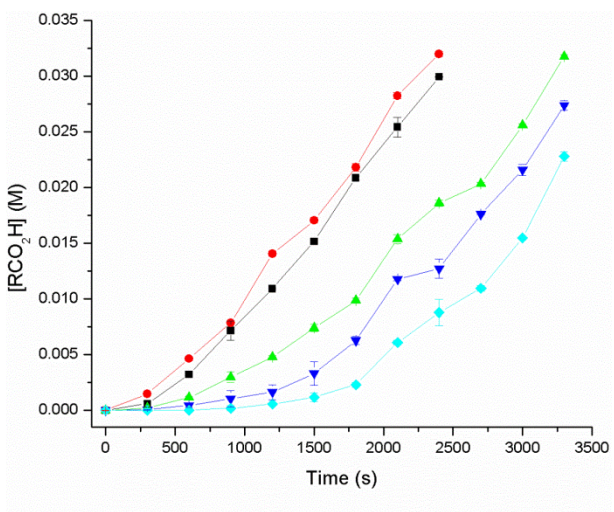


Figure S21. Carboxylic acid formation during the inhibited autoxidation of light paraffin oil at 160°C, initiated by 5.0 mM tetralin hydroperoxide, uninhibited without additives (■), or with 40 mM 2,4,6-tri-*tert*-butylpyridine (●), or inhibited with 40 μM bis(nitroxide) 2 with no additive (◆), 2 with 4.0 mM 2,4,6-tri-*tert*-butylpyridine (▼), or 2 with 40 mM 2,4,6-tri-*tert*-butylpyridine (▲).

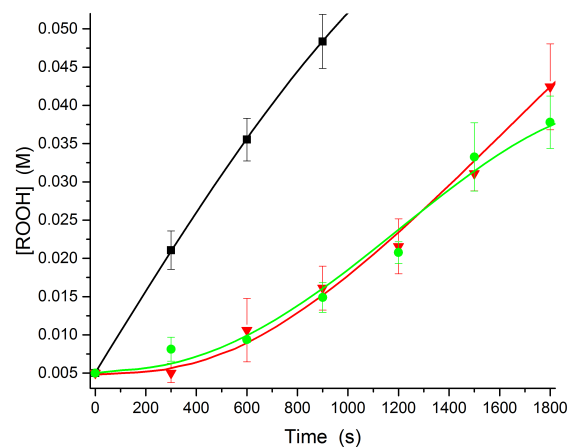
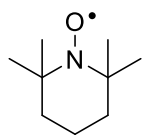


Figure 22. Hydroperoxide formation during the inhibited autoxidation of light paraffin oil at 160°C, initiated by 5.0 mM tetralin hydroperoxide, uninhibited without additives (■), or inhibited with 40 μM bis(nitroxide) **2** (▼) or with 40 mM of the bis(oxoammonium tetrafluoroborate salt) derived from **2** (●).

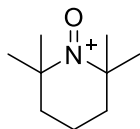
CBS-QB3 Computational Results and Structures



CBS-QB3 (0 K)=	-482.795331	CBS-QB3 Energy=	-482.783208
CBS-QB3 Enthalpy=	-482.782264	CBS-QB3 Free Energy=	-482.832096

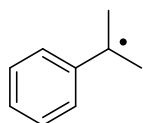
0 2

C	1.33321700	-0.06919700	-0.02995600
C	-1.33321700	-0.06919700	-0.02995600
C	-1.24567600	1.40132600	-0.48193500
C	0.00000000	2.12648100	0.02592400
C	1.24567600	1.40132600	-0.48193500
H	-1.24350400	1.43269500	-1.57766500
H	-2.15805100	1.91057200	-0.15640400
H	0.00000000	3.15965700	-0.33442700
H	0.00000000	2.18378900	1.11922500
H	1.24350500	1.43269500	-1.57766400
H	2.15805100	1.91057200	-0.15640300
N	0.00000000	-0.74664400	-0.20022700
C	1.76850600	-0.18385200	1.44528300
H	1.70922100	-1.22617600	1.76229500
H	2.80139000	0.15710900	1.55691500
H	1.14277600	0.41446000	2.10980900
C	2.33773500	-0.82266300	-0.91474100
H	3.32150000	-0.35212100	-0.83582500
H	2.41463100	-1.86414300	-0.60607000
H	2.02380200	-0.79745100	-1.96103100
C	-1.76850600	-0.18385100	1.44528300
H	-2.80139000	0.15711000	1.55691600
H	-1.70922100	-1.22617700	1.76229500
H	-1.14277500	0.41445900	2.10980900
C	-2.33773500	-0.82266300	-0.91474000
H	-2.41463100	-1.86414300	-0.60606900
H	-3.32150000	-0.35212200	-0.83582500
H	-2.02380200	-0.79745200	-1.96103100
O	0.00000000	-2.01663600	-0.04332700



CBS-QB3 (0 K)= -482.540989 CBS-QB3 Energy= -482.528794
 CBS-QB3 Enthalpy= -482.527850 CBS-QB3 Free Energy= -482.577353

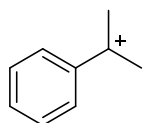
1 1			
C	1.36988900	-0.07079700	0.00983700
C	-1.36988900	-0.07079700	0.00983700
C	-1.25179400	1.33700600	-0.61215200
C	0.00000000	2.10829400	-0.20032400
C	1.25179500	1.33700600	-0.61215200
H	-1.27723100	1.23801900	-1.70204400
H	-2.15873100	1.87640700	-0.32786300
H	0.00000000	3.07875400	-0.70144700
H	0.00000100	2.32460500	0.87125200
H	1.27723000	1.23801900	-1.70204400
H	2.15873200	1.87640700	-0.32786400
N	0.00000000	-0.78133600	-0.11530400
C	1.69114300	-0.02779100	1.52441100
H	1.62103000	-1.01984900	1.97366800
H	2.72621300	0.30819200	1.61187200
H	1.06401300	0.66668500	2.07846500
C	2.39928900	-0.93253600	-0.72344100
H	3.34523200	-0.38815500	-0.71565100
H	2.55671200	-1.89550900	-0.23934900
H	2.11555500	-1.10129000	-1.76418900
C	-1.69114400	-0.02779100	1.52441100
H	-2.72621400	0.30819000	1.61187100
H	-1.62102800	-1.01984800	1.97366900
H	-1.06401500	0.66668700	2.07846500
C	-2.39928900	-0.93253600	-0.72344100
H	-2.55671200	-1.89550800	-0.23935000
H	-3.34523100	-0.38815400	-0.71565200
H	-2.11555400	-1.10129000	-1.76418900
O	0.00000000	-1.95292000	-0.29680100



CBS-QB3 (0 K)=	-348.837138	CBS-QB3 Energy=	-348.827927
CBS-QB3 Enthalpy=	-348.826982	CBS-QB3 Free Energy=	-348.872592

0 2

C	0.00005100	0.18619600	0.00000000
C	0.00003000	-0.56298500	1.21055100
C	-0.00006000	-1.94815000	1.20468200
C	-0.00011700	-2.65646200	0.00000000
C	-0.00006000	-1.94815000	-1.20468200
C	0.00003000	-0.56298500	-1.21055100
H	0.00008300	-0.04321500	2.16025700
H	-0.00008600	-2.48586500	2.14687000
H	-0.00021200	-3.74024300	0.00000000
H	-0.00008600	-2.48586500	-2.14687000
H	0.00008300	-0.04321500	-2.16025700
C	0.00008100	1.61359000	0.00000000
C	0.00003000	2.38028300	-1.29293000
H	0.00001600	3.45652100	-1.11456200
H	0.87859500	2.14892900	-1.90933800
H	-0.87854800	2.14889400	-1.90931300
C	0.00003000	2.38028300	1.29293000
H	-0.87854800	2.14889400	1.90931300
H	0.87859500	2.14892900	1.90933800
H	0.00001600	3.45652100	1.11456200



CBS-QB3 (0 K)=	-348.591896	CBS-QB3 Energy=	-348.584395
CBS-QB3 Enthalpy=	-348.583450	CBS-QB3 Free Energy=	-348.624080

```

1 1
C      -0.00002500  0.17759900  0.00000000
C      -0.00001400 -0.55691800  1.22452700
C      -0.00001400 -1.93538000  1.21932300
C      -0.00001600 -2.62579200  0.00000000
C      -0.00001400 -1.93538000 -1.21932300
C      -0.00001400 -0.55691800 -1.22452700
H      -0.00001100 -0.03416800  2.17143400
H      -0.00001200 -2.48409900  2.15251500
H      -0.00001400 -3.71002300  0.00000000
H      -0.00001200 -2.48409900 -2.15251500
H      -0.00001100 -0.03416800 -2.17143400
C      -0.00003000  1.59279100  0.00000000
C      0.00004000  2.36967100 -1.27175200
H      0.00009300  3.44185100 -1.09400600
H      0.87659000  2.11665400 -1.87916200
H     -0.87651200  2.11674400 -1.87919500
C      0.00004000  2.36967100  1.27175200
H     -0.87651200  2.11674400  1.87919500
H      0.87659000  2.11665400  1.87916200
H      0.00009300  3.44185100  1.09400600

```

References

- 1) Ikeda, H.; Hoshi, Y.; Namai, H.; Tanaka, F.; Goodman, J. L.; Mizuno, K. *Chem. Eur. J.* **2007**, *13*, 9207–9215.
- 2) Hanthorn, J. J.; Synthesis, Thermodynamic and Kinetic Studies of Novel Diarylamine Antioxidants & Development of a Fluorescent Probe for Quantifying Hydroperoxides and Measuring H-Atom Transfer Kinetics with Peroxyl Radicals. Ph.D. dissertation. Queen's University, Kingston, ON. 2012.
- 3) Holan, M.; Jahn, U. *Org. Lett.* **2014**, *16*, 58–61.
- 4) Connolly, T. J.; Baldoví, M. V.; Mohtat, N.; Scaiano, J. C. *Tetrahedron Lett.* **1996**, *37*, 4919–4922.
- 5) Mendes, P. *Trends Biochem. Sci.* **1997**, *22*, 361–363.
- 6) Howard, J. A.; Ingold, K. U. *Can. J. Chem.* **1965**, *43*, 2729–2736.
- 7) Maillard, B.; Ingold, K. U.; Scaiano, J. C. *J. Am. Chem. Soc.* **1983**, *105*, 5095–5099.
- 8) Litwinienko, G.; Ingold, K. U. *J. Org. Chem.* **2005**, *70*, 8982–8990.
- 9) Chateaufneuf, J.; Luszytk, J.; Ingold, K. U. *J. Org. Chem.* **1988**, *53*, 1629–1632.
- 10) Amorati, R.; Pedulli, G. F.; Pratt, D. A.; Valgimigli, L. *Chem. Commun.* **2010**, *46*, 5139–5141.
- 11) McClelland, R. A.; Kanagasabapathy, V. M.; Banait, N. S.; Steenken, S. *J. Am. Chem. Soc.* **1991**, *113*, 1009–1014.
- 12) Ohkatsu, Y.; Fujiwara, T.; *J. Japan Petroleum Inst.* **2007**, *50*, 87–93.
- 13) Willenbacher, J.; Wuest, K. N. R.; Mueller, J. O.; Kaupp, M.; Wagenknecht, H.; and Barner-Kowollik, C. *ACS Macro Lett.*, **2014**, *3*, 574–579.
- 14) Cohen, S. G.; Groszos, S. J.; Sparrow, D. B. *J. Am. Chem. Soc.*, **1950**, *72*, 3947–3951.
- 15) Shelton, J. R.; Liang, C. K. *Synthesis*, **1971**, 204–205.